THE JOURNAL OF BIOLOGICAL CHEMISTRY Vol. 278, No. 33, Issue of August 15, pp. 30569–30577, 2003

Printed in U.S.A.

Domain Truncation Studies Reveal That the Streptokinase-Plasmin Activator Complex Utilizes Long Range Protein-Protein Interactions with Macromolecular Substrate to Maximize Catalytic Turnover*

Received for publication, April 11, 2003, and in revised form, May 20, 2003
Published, JBC Papers in Press, May 27, 2003, DOI 10.1074/jbc.M303799200

Vasudha Sundram‡, Jagpreet S. Nanda‡, Kammara Rajagopal, Jayeeta Dhar, Anita Chaudhary§, and Girish Sahni¶

From the Institute of Microbial Technology, Chandigarh 160036, India

To explore the interdomain co-operativity during human plasminogen (HPG) activation by streptokinase (SK), we expressed the cDNAs corresponding to each SK domain individually (*α*, *β*, and *γ*), and also their two-domain combinations, *viz.* *αβ* and *βγ* in *Escherichia coli*. After purification, *α* and *β* showed activator activities of approximately 0.4 and 0.05%, respectively, as compared with that of native SK, measured in the presence of human plasmin, but the bi-domain constructs *αβ* and *βγ* showed much higher co-factor activities (3.5 and 0.7% of native SK, respectively). Resonant Mirror-based binding studies showed that the single-domain constructs had significantly lower affinities for "partner" HPG, whereas the affinities of the two-domain constructs were remarkably native-like with regards to both binary-mode as well as ternary mode ("substrate") binding with HPG, suggesting that the vast difference in co-factor activity between the two- and three-domain structures did not arise merely from affinity differences between activator species and HPG. Remarkably, when the co-factor activities of the various constructs were measured with microplasminogen, the nearly 50-fold difference in the co-factor activity between the two- and three-domain SK constructs observed with full-length HPG as substrate was found to be dramatically attenuated, with all three types of constructs now exhibiting a low activity of approximately 1–2% compared to that of SK·HPN and HPG. Thus, the docking of substrate through the catalytic domain at the active site of SK-plasmin(ogen) is capable of engendering, at best, only a minimal level of co-factor activity in SK·HPN. Therefore, apart from conferring additional substrate affinity through kringle-mediated interactions, reported earlier (Dhar *et al.*, 2002; *J. Biol. Chem.* 277, 13257), selective interactions between all three domains of SK and the kringle domains of substrate vastly accelerate the plasminogen activation reaction to near native levels.

Streptokinase (SK)[1] is a widely used bacterial thrombolytic protein that is secreted by several species of β-hemolytic streptococci (1, 2). It consists of a single polypeptide chain of 414 residues and is organized into three structurally similar, independently folding domains (termed α, β, and γ in order from N to C terminus of the polypeptide) that are separated by coiled coils and small flexible regions at the two ends (3–5). Like several other well known thrombolytic proteins, such as urokinase and tissue-plasminogen activator, SK exerts its effects through the conversion of human plasminogen (HPG) to its proteolytically active form, plasmin (HPN). Thus, during the treatment of various circulatory disorders, *e.g.* myocardial infarction, deep vein thrombosis, pulmonary embolism, etc., HPN generated by the activation of HPG helps restore blood flow to the afflicted part by proteolytic dissolution of the fibrin in the pathological clot. In contrast to tissue-plasminogen activator and urokinase, which are intrinsically HPG-specific proteases and thus "directly" act on HPG, SK is an enzymatically inert protein (6). However, it recruits circulating HPG to generate HPG activating potential; SK first combines with "partner" HPG in an equimolar manner to form a tight, enzymatically active complex, the so-called SK·HPG "virgin" activator complex (7, 8), which rapidly converts into a SK·HPN complex. The mature SK·HPN activator complex then catalytically transforms "substrate" molecules of HPG to HPN (1).

Plasmin is essentially a protease with a trypsin-like side chain specificity and broad substrate specificity. Free HPN cannot activate substrate HPG to HPN, but once combined with SK, the hitherto "nonspecific" active site of HPN becomes inordinately specific for the cleavage of the Arg^{561}-Val^{562} scissile peptide bond in substrate HPG (9). This remarkable alteration of the macromolecular substrate specificity of HPN by SK as a result of the latter's "protein co-factor" property, which has been a subject of intense investigations, is currently thought to be due to exosites generated on the SK·HPN activator complex, as demonstrated recently by the elegant use of active site-labeled fluorescent HPN derivatives (10). Deciphering the molecular details of the mechanism and associated structure-function co-relations whereby SK modulates the substrate preference of the active site of plasmin(ogen) after complexation with the latter is undoubtedly vital to the successful design of improved SK-based thrombolytic proteins of the future (11, 12). However, the fact that both participants are complex, multi-domain proteins: SK, with its three structurally homologous domains (3–5), and HPG, composed of a catalytic and five kringle domains (1, 13), greatly compounds the struc-

* This work was supported by generous grants from the Department of Biotechnology and the Council of Scientific and Industrial Research, Government of India. The costs of publication of this article were defrayed in part by the payment of page charges. This article must therefore be hereby marked "*advertisement*" in accordance with 18 U.S.C. Section 1734 solely to indicate this fact.

‡ Both authors contributed equally to this work.

§ Present address: Dept. Environmental Sciences, Indian Agricultural Research Institute, Pusa, Dr. K. S. Krishnan Marg, New Delhi 110012, India.

¶ To whom correspondence should be addressed: Inst. of Microbial Technology, Sector 39-A, Chandigarh 160036, India. Fax: 91-172-690585 or 91-172-690632; E-Mail: sahni@imtech.res.in.

[1] The abbreviations used are: SK, streptokinase; nSK, native-like streptokinase; HPG, human plasminogen; HPN, human plasmin; μPG, microplasminogen; EACA, ϵ-amino caproic acid; SAK, staphylokinase.

ture-function challenges involved in solving this question. The crystal structure of SK complexed with microplasmin (the catalytic protease domain of HPN, devoid of its five kringle domains) has provided insights regarding the molecular mechanism whereby SK manages to switch the substrate specificity of the active site of HPN (5), indications of which had also been gleaned earlier through solution studies (14, 15). These studies indicate that SK acts as a protein co-factor of the plasmin active site by forming a "three-sided valley" around the active center by virtue of its tri-domain structure. Thus, it has been postulated that the docking of the catalytic subunit of HPG onto the activator complex by protein-protein interactions facilitates cleavage of the scissile peptide bond in the macromolecular substrate by an otherwise nonspecific active site (5). However, the crystal structure does not provide any indication of whether the kringle domains of the substrate play any role in this process.

In contrast to the three-domain structure of SK, staphylokinase (SAK), another functionally similar, "indirect" HPG activator protein but one that has a single domain only, also operates by docking substrate HPG into the active center of its binary complex with plasmin(ogen) (16). Although SAK displays little sequence similarity with SK, its single domain bears a remarkable conformational similarity with one of the three SK domains in particular (the α domain) and all three domains of SK in general, which, in turn, are structurally homologous to each other (17). However, the SAK·HPN activator complex is known to possess a significantly lower catalytic efficiency than SK·HPN (18, 19). Apart from the single-domain prototypic structure of SAK, another mechanistically similar plasminogen activator from *Streptococcus uberis* (abbreviated SUPA) has also been isolated that possesses a two-domain structural motif (20, 21). Thus, a compelling need exists to glean insights regarding the similarities and dissimilarities in the "design principles" between the three-domain SK, on the one hand, and the single- and two-domain structures of SAK and SUPA on the other, particularly in terms of the structure-function co-relations that underlie the interdomain co-operativity between the individual SK domains.

Taking a minimalist approach, a pertinent question that can be posed in the above context is whether any of the isolated domains of SK also possess, like the single domain of SAK, the ability to bind with HPG in both substrate and partner modes and, if the answer is affirmative, whether this binding is functionally translated into a capability, even if highly compromised compared with native SK, to switch the nonspecific substrate preference of partner plasmin to that of a HPG activator enzyme. A recent study (22) has attempted to address this issue, particularly in terms of the functional properties of single SK domains, and elegantly demonstrated the presence of detectable, albeit very low levels of HPG activator activity in two of the three SK domains. The results of this study also stimulate curiosity about the possibility of a hierarchical generation of catalytic activity in SK (*i.e.* the possible existence of a progressive increase in co-factor activity from the single- to two-domain, and finally, to the three-domain native motif) and the need to gain meaningful insights into the design principle(s) selected by evolution for plasminogen activators of bacterial origin. As a first step in this direction, in the present study we have therefore expressed each of the three domains of SK, as well as their two-domain combinations (*viz.* $\alpha\beta$ and $\beta\gamma$) in a heterologous expression system and compared their catalytic and binding properties both against full-length macromolecular substrate, HPG as well as its kringle-less derivative, microplasminogen (μPG). Thus, with this approach, we have attempted to explore the interdomain co-operation prevalent in SK, as well as between the SK·HPG activator complex and substrate HPG. The results presented below reveal that the kringle domains of substrate help not only in substrate docking, as proposed recently (23, 24), but also in substrate turnover, even though they are distinctly apart from the immediate microenvironment of the "target" scissile peptide bond, the specific region of the substrate polypeptide that is selectively cleaved during plasminogen activation.

EXPERIMENTAL PROCEDURES

Materials

HPG was either purchased from Roche Applied Science or purified from human plasma by affinity chromatography (25). The cloning vector pBluescript II KS$^-$, thermostable DNA polymerase (*Pfu*) and *Escherichia coli* strain XL-Blue were procured from Stratagene Inc. (La Jolla, CA). All other enzymes used for genetic manipulation were obtained from New England Biolabs (Beverly, MA). The oligonucleotide primers were either synthesized in-house on an Applied Biosystems DNA synthesizer model 492 or custom-synthesized by Ransom Hill Biosciences Inc. (Ramona, CA). DEAE-Sepharose (Fast-flow) and Chelating Sepharose were procured from Amersham Biosciences, and phenyl-agarose for hydrophobic interaction chromatography was purchased from Affinity Chromatography Ltd. The T7 RNA polymerase promoter-based expression vector, pET-23d and Bug buster® (a commercial reagent for rapid bacterial cell lysis) were procured from Novagen Inc. (Madison, WI). All other chemicals used were of the best commercial grade available.

Expression and Purification of SK from E. coli

The plasmid construct for the intracellular expression of SK in *E. coli* (pET-23d-SK) under the control of the T7 phage RNA polymerase promoter has been described (26). Briefly, the purification involved lyzing the cells by sonication followed by ammonium sulfate precipitation (60% saturation) and two chromatographic steps, *viz.* hydrophobic interaction chromatography on phenyl-agarose and anion exchange chromatography. This yielded homogeneous SK with an overall yield of 55–60% with a specific activity of 1.1×10^5 IU/mg protein (27).

Cloning of Single and Bi-domains of SK

The exact boundaries of individual domains were selected based on limited proteolysis data (4), which also cross-correlated well with the limits defined by the crystal structure of SK (5). The sequences 1–143 and 143–293 were chosen to represent the α domain and the β domain, respectively (4). The γ domain (SK293–414) was cloned from the region coding for residues 300–387, because the C-terminal end of the γ domain (residues 388–414) contains residues that are not critical for the functioning of full-length SK and forms a disorganized and flexible segment that undergoes rapid degradation in the presence of HPN (4, 5, 28, 29).

The construction of the truncated derivatives of SK was carried out by PCR amplification of the desired sequence, using SK as template, and specific upstream and downstream primers that also contained specific restriction endonuclease (RE) sites to allow for facile, directional docking of the amplified fragment into pET-23d-SK. Primers for the construction of the α domain were as follows: upstream primer, 5′-AGCCAATTAGACGTCAGCGTTGCAGAAACTGTTGAGG-3′, and downstream primer, 5′-ATCTTGCTCGAGAACGCGCACATGTCCACTTAGCAA-3′. Primers for the construction of the β domain were as follows: upstream primer, 5′-TCAGCCATGGTTAGACCATATAAA-3′, and downstream primer, 5′-ATGGGGATCCTATTTCAAGTGACTGCGATCAAAGGG-3′. Primers for the construction of the γ domain were as follows: upstream primer, 5′-ATACCATGGTTGATGTCGATACTAATGAA-3′, and downstream primer, 5′-TTGCTCGAGGGCTAAATGATAGCTGGCATTCTC-3′. Construct $\alpha\beta$ was prepared as follows: The "vector" DNA fragment obtained after digestion of pET-23d-β with the REs *Bgl*II and *Bse*RI was ligated with the "insert" fragment obtained from the digestion of pET-23d-SK with the same REs. Primers for the construction of $\beta\gamma$ were as follows: upstream primer, 5′-TCAGCCATGGTTAGACCATATAAA-3′, and downstream primer, 5′-ATAGGCTAAATGATAGCTAGCATTCTCTCCTTC-3′.

Purification of His_6-tagged α and γ Domains Using Metal Affinity Chromatography

The single-domain constructs, α as well as γ, were expressed as proteins with His_6 tag extensions at their C termini to aid their purification by affinity chromatography on Ni^{2+}-immobilized metal affinity

chromatography (30). The α domain was found predominantly in the form of inclusion bodies, whereas the γ domain remained soluble in the intracellular milieu of *E. coli*. Hence, inclusion bodies of the α domain obtained after lyses of the cells with Bug buster reagent were first dissolved in 8 M urea. The inclusion bodies of the α domain dissolved in 8 M urea and the soluble γ domain obtained after cell lysis were further diluted 15-fold in 50 mM sodium phosphate buffer (pH 7.5) containing 10 mM imidazole and 250 mM NaCl before loading on the immobilized metal affinity chromatography matrices. Successive washes with 50 mM sodium phosphate buffer (pH 7.5) containing 60 mM imidazole and 250 mM NaCl were given to remove unwanted, loosely bound proteins, and the His-tagged proteins were finally eluted with 50 mM sodium phosphate buffer (pH 7.5) containing 250 mM imidazole and 250 mM NaCl.

Purification of β Domain of SK

The β domain of SK (residues 143–293) was expressed in *E. coli* as a soluble protein at a level ~30% of the total soluble protein fraction and was purified as described earlier (23).

Purification of the Two-domain Constructs αβ (SK 1–293) and βγ (SK 143–414)

The covalently contiguous two-domain construct, αβ, was expressed as a soluble protein in *E. coli* BL-21 cells, whereas the βγ protein was expressed predominantly as inclusion bodies. The purification involved lyzing the cells by sonication followed by ammonium sulfate precipitation (60% saturation) and two tandem chromatographic steps, namely hydrophobic ion chromatography on phenyl-agarose and ion exchange chromatography on DEAE-Sepharose (Fast-flow) essentially as described for SK above. The eluted fractions contained protein that was more than 95% pure as analyzed by SDS-PAGE.

Circular Dichroic Analysis of nSK/SK Domains

Far-UV CD spectra of SK/SK domains (concentration 0.15 mg/ml in phosphate-buffered saline, pH 7.2) were recorded on a Jasco-720 spectropolarimeter. Measurements were carried out from 190 to 250 nm in a 0.1-cm-pathlength cuvette, and the appropriate buffer base line was subtracted from the protein spectra. The final spectrum analyzed was an average of 10 scans. Secondary structure analysis to compute the content of α helix, β sheet, random coil, and other secondary structure(s) were carried out using the algorithm described by Yang *et al.* (31).

Preparation of Microplasminogen

Microplasminogen, the catalytic domain of plasminogen (residues Lys^{539}–Asn^{790}), devoid of all the kringles was prepared by cleavage of HPG by HPN under alkaline conditions (0.1 N glycine/NaOH buffer, pH 10.5, 10:1 ratio of HPG and HPN) at 30 °C. Microplasminogen was purified from the reaction mixture by passing through a Lys-Sepharose column (Amersham Biosciences), followed by a Soyabean-trypsin inhibitor-Sepharose CL-4B column to absorb HPN and microplasmin, as reported (23, 32). The flow-through was then subjected to molecular sieve chromatography, after concentration by ultrafiltration, on a column (16 × 60 cm) of Superdex-75™ (Amersham Biosciences). The purity of μPG formed was analyzed by SDS-PAGE, which showed a single band moving at the position expected from its molecular size (32), and the identity of the protein was confirmed by N-terminal protein sequencing. Activation with urokinase, which is known to be an efficient activator of μPG despite the absence of kringle domains in the latter, was used to establish that the rate of activation of this preparation, when used as substrate, was comparable with that obtained when using SK·HPN as the activator species.

Assay for Detection of Extremely Low HPG Activation Capability

Catalytic amounts of domains were added to the assay buffer (100 mM Hepes, pH 7.5) containing 2 μM of HPG and chromogenic substrate (0.5 mM), and the change in absorbance was monitored spectrophotometrically at 405 nm as a function of time at 22 °C (Pathway I). To detect intrinsically low HPG activation capability in single-domain/bi-domain construct(s) that may otherwise not be capable of activating the partner HPG unless provided with a preformed active site (*i.e.* only Pathway II capability), equimolar complexes of HPN and the SK derivative were premixed on ice for 1 min, and catalytic amounts were withdrawn and added to 2 μM HPG and chromogenic peptide substrate in the assay buffer containing 100 mM Hepes (pH 7.5) in case of single-domain proteins and 50 mM Tris-Cl (pH 7.5) in case of the two-domain proteins. The reactions were recorded spectrophotometrically at 405 nm, and the progress curves obtained from corresponding control reactions (containing HPG and same amounts of HPN but no domain) were subtracted from the test reactions. The resultant curves so obtained were used to determine the rate of HPG activation, which was then expressed as a percentage of activity, relative to SK. The initial phase (0–8 min) was generally used for this calculation in both cases, to overcome any loss of activity at later stages caused by possible proteolytic stability.

To establish whether the isolated domains had genuine activator activities over and above that associated with the background cells, *E. coli* BL21 cultures transformed with the pET-23d vector but not containing any domain-encoding insert, after induction with isopropyl-1-thio-β-D-galactopyranoside, were harvested and lyzed similarly to ones prepared for purifying the individual domain(s). These cell lysates were subjected to exactly the same treatments as the ones prepared from cultures harboring plasmids for α, β, or γ, including immobilized metal affinity chromatography and desalting steps. The fractions from "control" columns (on which the lysates containing just the expression plasmids without any SK domain insert were processed) identical in volume to the corresponding eluted protein fractions from the "test" columns (from which the domains were being purified) were collected in parallel and were then used for assessing HPG activator activity. The control fractions, which served to measure the background *E. coli* cell-associated HPG activator activity consistently, showed a very low level of activity (<0.005%) but one that was significantly lower than the activity observed with any of the truncated domain constructs.

Determination of Kinetic Constants for HPG Activator Activity

Varying amounts of HPG were added to the assay cuvette containing fixed amounts of single-domain or bi-domain constructs and chromogenic substrate (0.5 mM), and the change in absorbance was monitored at 405 nm as a function of time at 22 °C. Also, the kinetics of HPG activation by the activator complexes were measured by transferring suitable aliquots of preformed complexes (single-domain or bi-domain constructs, and HPN) to the assay cuvette containing different concentrations of substrate HPG. To compute the k_{cat}, the number of functional HPN active sites was determined by titration with an active site acylating reagent, *p*-nitrophenyl *p*-guanidinobenzoate (7, 33, 34).

Kinetic Analysis of Protein-Protein Interactions Using Resonant Mirror Technology

Binary Interaction Analysis—Association and dissociation between HPG and the nSK/SK domains, *viz*. bi-domains (αβ and βγ) and single-domains (α and β) referred to hereafter as binary interaction, were followed in real time by Resonant Mirror-based detection using IAsys Plus™ system (Cambridge, UK) (35, 36). In these experiments, streptavidin was captured on biotin cuvettes. This was followed by the attachment of biotinylated HPG to the streptavidin captured on the cuvette. Nonspecifically bound HPG was then removed by repeated washing with phosphate-buffered saline followed by three washes with 10 mM HCl. The net response chosen for the immobilized biotinylated HPG onto the cuvette was 700–800 arc seconds in all the experiments. The experiments were performed at 25 °C in 50 mM phosphate-buffered saline (pH 7.4) containing 0.1% Tween 20, 250 mM NaCl, and 50 μM *p*-nitrophenyl *p*-guanidinobenzoate (binding buffer). The latter was included to prevent plasmin-mediated proteolysis.

After equilibrating the cuvette with binding buffer, varying concentrations of either nSK/SK domains were added, and each binding response was monitored during the "association" phase. Subsequently, the cuvette was washed with the binding buffer, and the "dissociation" phase was recorded (37). Following each cycle of analysis, the cuvette was regenerated by washing with 10 mM HCl, and the base line was re-established with the binding buffer. In parallel, in the control cell in the dual channel cuvette, immobilized streptavidin alone was taken as a negative control for the binding studies.

The data were analyzed after subtraction of the corresponding nonspecific refractive index component(s), and the kinetic constants were calculated from the sensorgrams by nonlinear fittings of association and dissociation curves using the software FASTfit™, supplied by the manufacturer. The dissociation rate constant (k_d) was calculated from the average of four dissociation curves obtained at saturating concentration of ligate. The equilibrium dissociation constant (K_D) was then calculated from the extent of association of monophasic curve. The k_a was calculated from the equation k_d/K_D. The values of K_D obtained using this relationship were in good approximation to those obtained by k_d/k_a obtained from the linear fit of k_{on} *versus* ligate concentration (38).

Ternary Interaction Analyses—A Resonant Mirror technology-based biosensor was also used to measure the rate and equilibrium dissocia-

tion constants describing interactions between soluble ligates (HPG and μPG) and nSK/SK domains complexed with immobilized HPG. In binary interaction studies, it was evident that when the soluble nSK/SK domain was added to the immobilized HPG, a rapid and avid nSK/SK domains·HPG (except single domains, α and β) binary complex formation occurs. The dissociation of these binary complexes is very slow because of the high stability of SK·HPG complex (23). After allowing the complex to dissociate maximally (~20 min), the dissociation base line becomes stable, which remains unaffected even after washing with 2.5 mM EACA. In case of single domains (α and β), weak binary complexation with immobilized HPG was observed, and it was seen that the dissociation rates in binding buffer itself were very high; thus, stable base lines as observed in the case of bi-domains and nSK were not observed.

Varying concentrations of either "ternary" HPG (0.1–1.0 μM) or μPG (1–6 μM) were then added to monitor the binding by recording the association phase. Subsequently, the cuvette was washed with the binding buffer three times, and the dissociation phase was then recorded. After each cycle of analysis, the original base line was reestablished by stripping off the undissociated ternary ligate with 2.5 mM EACA followed by three washes with binding buffer. It was earlier established (23) that EACA at this concentration completely abolishes the interaction of ternary HPG with the binary complex, whereas the binary complex remains stable. In experiments where μPG was used as the soluble ternary ligate, 1 mM EACA was found to be sufficient to strip off the undissociated μPG, whereas washing with binding buffer alone resulted in incomplete regeneration of the base line (23). Equilibrium dissociation constant(s) were determined by analysis of the extent of association as well as from k_d/k_a. Dissociation and association constants were calculated by the procedure similar to the one followed in case of binary interaction analysis.

RESULTS AND DISCUSSION

Isolation and Characterization of Isolated Single and Bi-domains of SK—To measure the HPG activator activities in isolated domains and bi-domains of SK of *Streptococcus equisimilis*, each of the three isolated domains (α, SK1–143; β, SK143–293; and γ, SK300–387) and bi-domain constructs (αβ and βγ) were constructed by PCR amplification of cDNAs encoding for respective domains followed by cloning in pET-23d, a T7 phage RNA polymerase promoter-based vector (26). All of these constructs were then expressed in *E. coli* BL21 (DE3) cells. Good expression levels were observed for all of these constructs, and purification strategies for each of them were then standardized (see "Experimental Procedures") to obtain preparations with purity levels well over 95% as judged by SDS-PAGE (Fig. 1*A*). The secondary structure content of the isolated single- and double-domain derivatives was determined using far-UV CD measurements (Fig. 1*B*). The secondary structural features of the SK derivatives indicated that they were folded, because they were found to be largely in concordance with the reported data in literature, either based on spectroscopic analysis (4, 28) or that expected from direct x-ray structural data on SK domains (5, 39, 40).

Substrate HPG activation by SK can proceed along two Pathways (41). The first is Pathway I, wherein, after a high affinity complexation occurs between SK and partner HPG molecule, a virgin site is formed in the zymogen in absence of any proteolytic cleavage (7, 8). However, this complex rapidly converts to SK·HPN, the activator species that catalytically activates molecules of substrate HPG, after the partner HPG has been proteolytically converted to plasmin. In Pathway II, SK can directly complex with active HPN and then can activate substrate HPG. Mutants of SK that are impaired in Pathway I capability can sometimes activate substrate HPG through pathway II if "supplied" with a preformed, partner active site in the form of HPN (22). Thus, zymogen activation of partner HPG by SK under Pathway I and the conversion of macromolecular substrate specificity of the HPN active site upon the latter's complexation with SK constitute two distinct (although

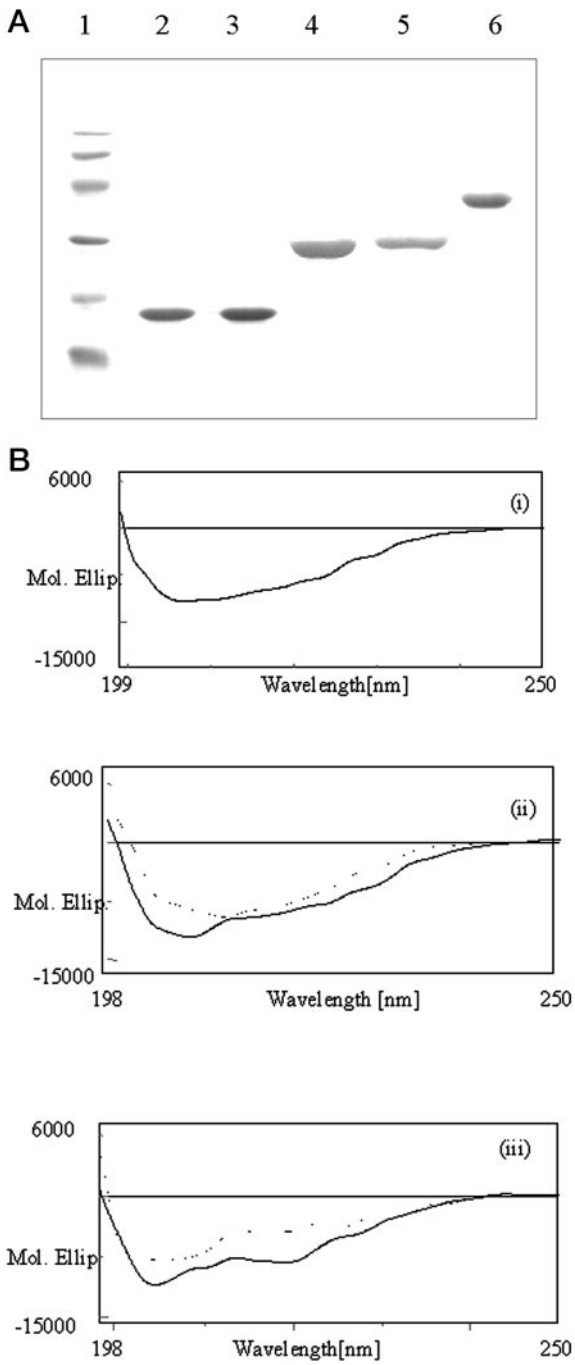

FIG. 1. *A*, SDS-PAGE analysis of purified SK/SK domains. Purified proteins were electrophoresed on 15% SDS-PAGE gels and stained with Coomassie Blue R-250 dye. *Lane 1*, molecular mass markers (from *top* to *bottom*, 97, 66, 45, 31, 21.5, and 14 kDa); *lane 2*, α domain; *lane 3*, β domain; *lane 4*, αβ domain; *lane 5*, βγ domain; *lane 6*, nSK. *B*, far-UV CD spectra of SK domains. The far-UV CD spectra in the wavelength range of 197–250 nm was determined as outlined under "Experimental Procedures." The curves shown are nSK (*i*), αβ (*solid line*) and βγ (*dotted line*) (*ii*), and α (*dotted line*) and β domains (*solid line*) (*iii*).

partially overlapping) biochemical properties of HPG activation with this activator protein.

We first examined the functional ability of purified individual (single) domains to activate substrate HPG using either excess HPG (Pathway I) or with excess substrate HPG after premixing with equimolar amounts of HPN (Pathway II). The γ-domain did not show any detectable activator/co-factor activity under either of these assay conditions, but in the case of α and β domains, apparent activator activities that could be

TABLE I
Steady state kinetic parameters for HPG activation by equimolar complexes of HPN and nSK/SK domains

The kinetic parameters for co-factor activity against HPG as substrate were determined with the respective activator complexes at 22 °C as described under "Experimental Procedures." The data represent the means of three independent determinations.

Activator species	K_m	k_{cat}	k_{cat}/K_m
	μM	min^{-1}	$min^{-1}\ \mu M^{-1}$
nSK·HPN	0.5 ± 0.1	11 ± 0.5	22
$\alpha\beta$·HPN	0.6 ± 0.2	0.33 ± 0.1	0.55
$\beta\gamma$·HPN	0.6 ± 0.2	0.08 ± 0.02	0.133
α·HPN	2.0 ± 0.5	0.049 ± 0.02	0.025
β·HPN	ND[a]	0.005 ± 0.003	ND

[a] ND, could not be accurately determined because of the intrinsically low level of co-factor activity.

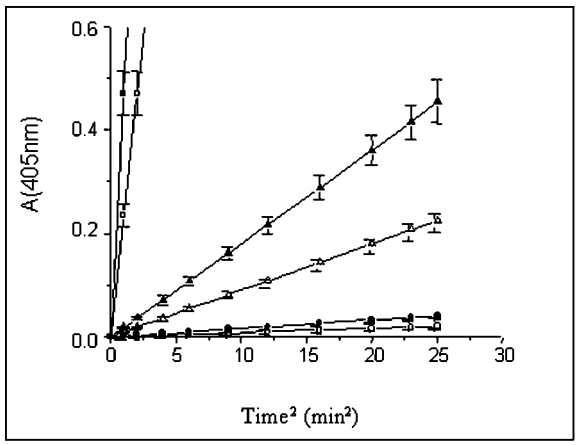

FIG. 2. **Activation of substrate HPG by SK and individual domains of SK.** The figure shows progress curves (405 nm *versus* time^2) for substrate HPG activation by catalytic amounts of activator complexes of nSK or different derivatives of SK complexed with HPN. An equimolar complex of nSK and HPN (0.5 μM each) was prepared over ice and kept for 1 min, and catalytic amounts of the complex (1 nM, *solid squares*; 0.5 nM, *open squares*) were added to the assay cuvette already containing HPG (2 μM) and chromogenic substrate (0.5 mM). The reaction was then monitored spectrophotometrically at 405 nm over time. Similarly, an equimolar complex of $\alpha\beta$ and HPN (0.5 μM each) was prepared, and different amounts of the complex (1 nM, *solid triangles*; 0.5 nM, *open triangles*) were added into the assay cuvette having chromogenic substrate (0.5 mM) and substrate HPG (2 μM). The reaction was then monitored spectrophotometrically at 405 nm. Substrate HPG activation by α domain is also shown. An equimolar mixture with HPN (0.5 μM each) was prepared and incubated on ice for 1 min, following which varying amounts (1 nM, *solid circles*; 0.5 nM, *open circles*) were then added to the assay cuvette containing HPG (2 μM) and chromogenic substrate (0.5 mM). All of the reactions were carried out at 25 °C.

detected using HPG alone were not more than 0.002% as compared with the corresponding activity with SK, taken as 100%. These results are very similar to those reported by Loy *et al.* (22). However, the barely perceptible activator activity associated with α and β were found to be strongly HPN-dependent, because the addition of small amounts of HPN in the assay mixtures resulted in sharp enhancement of HPG activation rates (data not shown); indeed when activator activity of α domain against substrate HPG was measured after premixing with HPN, it was found to increase dramatically by several orders of magnitude compared with its activity measured directly with HPG. The α domain now exhibited an activity ~0.5% that of native SK, whereas the β domain also showed enhanced activity of approximately 0.05% compared with SK (Table I, which shows the steady-state kinetic data for HPG activation). However, it is clear that despite the availability of preformed HPN as partner, the co-factor activities of both the single domains remained, at best, a small fraction of that observed with native nSK.

The presence of relatively low co-factor activities in the isolated domains prompted us to examine whether two-domain combinations of SK acquired a greater capability for catalysis as compared with the single-domain constructs. The latter ($\alpha\beta$ and $\beta\gamma$) were therefore tested for their ability to activate substrate HPG in an HPN-independent or -dependent manner, as before. It was observed that, as with single-domains, $\alpha\beta$ and $\beta\gamma$ had very low activities in the absence of HPN (<0.05%), as compared with that of nSK, but in presence of HPN, significantly higher catalytic ability as compared with that seen with individual domains could be observed; $\alpha\beta$ and $\beta\gamma$ had approximately 3.5% and 0.7% co-factor activities in presence of HPN, respectively, as compared with that of nSK measured under similar conditions (see also Fig. 2 for comparative HPG activation progress curves of single- and two-domain constructs). The steady-state kinetic constants obtained with HPG as substrate for two-domain constructs are also shown in Table I along with those of single domains, all activities being measured after making 1:1 complexes with HPN prior to the assay in presence of excess substrate HPG. It may also be mentioned that equimolar mixtures of single domains or mixtures of two or three domains together did not result in any detectable enhancements in activity over those additively associated with the individual domains, indicating that the covalent contiguity between the individual domains in $\alpha\beta$ and $\beta\gamma$ contributed synergistically toward the acquisition of higher activities by the two-domain construct(s).

An analysis of the steady-state kinetic parameters shown in Table I indicates that although the two-domain molecules were minimally altered in K_m values for HPG (approximately 0.5 μM in case of nSK), they still exhibited a significantly reduced k_{cat} for HPG activation when compared with the native protein. In contrast, we observed a nearly 3–4-fold increase in K_m (~2 μM) for substrate HPG binding to activator complex in the case of the single domain, α, thereby indicating that the isolated domain had probably lesser affinity for substrate HPG in comparison with both full-length native nSK and the bi-domain derivatives. Although these data, together, clearly establish that there is a dramatic increase in the co-factor capability as the single domain(s) of SK acquire a two-domain character, the latter are still significantly compromised in terms of their catalytic power when compared with the three-domain, native format.

Interaction of Single and Bi-domain Constructs of SK with HPG—The inability of single- and bi-domain derivatives of SK to activate substrate HPG, even with HPN, beyond a certain low level prompted us to examine their capability (or lack thereof) to bind HPG. For this purpose, various real time binding parameters such as association and dissociation rate constants and equilibrium dissociation constants for binary interactions between immobilized biotinylated-HPG and nSK/SK domains were first determined by the Resonant Mirror approach using a real time molecular interaction system (IAsys Ltd.). The kinetic parameters so obtained for the binary interaction between immobilized HPG and nSK or those of single- (α and β) and bi-domain constructs ($\alpha\beta$ and $\beta\gamma$) are shown in Table II. It is clear from these results that the equilibrium dissociation constants (K_D) of $\alpha\beta$ (~2 nM) and $\beta\gamma$ (~7.5 nM) are not grossly different from that of nSK (~1.0 nM), whereas the K_D values of single domains (~100 nM) are nearly 2 orders of magnitude greater than that for nSK. These observations indicate that partner HPG binds to the bi-domains with nearly the same affinity as it binds to nSK, whereas single domains bind to partner HPG with considerably lesser affinity as compared with native nSK. It is thus possible that the lowered affinity between the single domain(s) and HPG may be a major

TABLE II

Association and dissociation rate constants and apparent equilibrium dissociation constants of partner and substrate HPG with SK/SK domains

Kinetic constants for the binary interaction between immobilized biotinylated HPG and nSK/SK domains and thereafter, kinetic constants for the ternary interaction of substrate HPG with nSK/SK domains were determined as outlined under "Experimental Procedures." The kinetic constants were determined by applying the FASTfit™ program to the binding data obtained using IAsys biosensor as described under "Experimental Procedures." A stable binary complex between nSK/SK domains and HPG immobilized onto the cuvette was made, and then the binding of varying concentrations of HPG (0.1–1 μM) was monitored.

Activator protein	Binary interaction of SK with partner HPG			Ternary interaction of binary complex with substrate HPG		
	k_a	k_d	K_D	k_a	k_d	K_D
	$M^{-1}\,s^{-1}$	s^{-1}	M	$M^{-1}\,s^{-1}$	s^{-1}	M
nSK	$5.8 \pm 0.5 \times 10^7$	$6.0 \pm 0.5 \times 10^{-2}$	$1.03 \pm 0.5 \times 10^{-9}$	$3 \pm 0.4 \times 10^5$	$3.6 \pm 0.3 \times 10^{-2}$	$0.12 \pm 0.05 = 10^{-6}$
$\alpha\beta$	$4.8 \pm 1.0 \times 10^7$	$9.6 \pm 1.5 \times 10^{-2}$	$2.0 \pm 0.5 \times 10^{-9}$	$3.9 \pm 0.5 \times 10^5$	$7.8 \pm 1.6 \times 10^{-2}$	$0.20 \pm 0.1 \times 10^{-6}$
$\beta\gamma$	$1.46 \pm 0.6 \times 10^7$	$8.7 \pm 1.0 \times 10^{-2}$	$6.0 \pm 1.5 \times 10^{-9}$	$2.5 \pm 1.1 \times 10^5$	$5.6 \pm 1.2 \times 10^{-2}$	$0.22 \pm 0.05 \times 10^{-6}$
α	$0.082 \pm 0.05 \times 10^7$	$9.2 \pm 2.0 \times 10^{-2}$	$112 \pm 10 \times 10^{-9}$	ND[a]	ND	ND
β	$0.11 \pm 0.03 \times 10^7$	$9.7 \pm 2.0 \times 10^{-2}$	$87 \pm 10 \times 10^{-9}$	ND	ND	ND

[a] ND, could not be accurately determined because of the intrinsically low level of co-factor activity.

contributive cause to their overall lowered co-factor activity. However, the native-like affinity observed for HPG in case of the two-domain constructs, particularly $\alpha\beta$, suggests that the underlying cause of their lowered co-factor activities does not likely reside at this level of intermolecular interaction.

After establishing the stability of binary complexes of the different constructs with immobilized HPG, ternary interactions between "substrate" HPG and different domains of nSK (single- and bi-domains) precomplexed with immobilized HPG were explored using, again, an approach based on the Resonant Mirror technique. The application of the Resonant Mirror technique for detecting and studying ternary interactions in the SK·HPG system has been reported recently (23). In this direct approach for analyzing the protein-protein interactions operative between macromolecular substrate and the SK·HPG activator complex, mildly biotinylated HPG is first immobilized onto the surface of a Resonant Mirror biotin-cuvette, onto which a thin film of streptavidin has earlier been layered, followed by washing with buffer to remove excess unbound HPG. The immobilized HPG is then "challenged" with SK to form equimolar SK·HPG complex. The binary complex so formed is washed extensively with buffer, a procedure against which the high affinity SK·HPG binary complex is fairly stable (23). To the binary complex is then added excess substrate HPG; the formation of a ternary HPG·SK·HPG complex can then be observed to give additional ternary signal over and above that obtained earlier at the binary complexation stage, as shown in Fig. 3 (see also Ref. 23). Thus, this assay, which is capable of monitoring in real time, the "docking" of substrate HPG onto the preformed SK·HPG binary complex can be utilized to explore altered substrate-interacting capability, if present, in a SK derivative/mutant after prior complexation with partner HPG. In the past, we have successfully employed this approach to demonstrate affinity changes between the SK-plasmin(ogen) activator complex and its altered form for the macromolecular substrate, HPG (23). When this assay was carried out in the present study (see "Experimental Procedures" for details), it was observed that the equilibrium dissociation constant (K_D) of the ternary interaction of substrate HPG with bi-domains of nSK (*viz.* $\alpha\beta$ and $\beta\gamma$) was similar to that of native SK for substrate HPG (~0.12 μM). The association rate constant (k_a) and dissociation rate constant (k_d) of ternary interactions between both the bi-domain of nSK and substrate HPG were found to be nearly similar to that observed in case of ternary interaction of substrate HPG with native full-length nSK (Tables I and II). However, in case of the single domains (α and β), real time kinetic constants for ternary complexation could not be determined at all essentially because of the weak nature of binary complex formation, in the first place, between the isolated domain(s) and immobilized HPG (Fig. 3*C*). This was so because, in this case, although the binary complex(es) could be observed when much higher HPG concentrations than those required for nSK were employed, they were seen to dissociate rapidly even by moderate buffer washing, conditions under which the native SK·HPG was stable. In contrast to single domains, however, the results of Resonant Mirror studies on $\alpha\beta$ and $\beta\gamma$ clearly demonstrate that they seem to be as capable of docking macromolecular substrate as the native tri-domain nSK molecule.

Taken together, the steady-state kinetics and real time physico-chemical studies of substrate HPG interaction with nSK/SK domains clearly establish that although substrate HPG docks with both the bi-domain derivatives of SK with nearly the same affinity as that with full-length SK, this near-native docking of substrate HPG is not proportionately translated into a nearly native co-factor activity in either of the two bi-domain derivatives, and the native three-domain structure is catalytically the most effective in terms of catalytic turnover. The lack of any significant quantitative co-relation in a given derivative between the docking ability of substrate on the one hand and its subsequent catalytic turnover on the other strongly indicated that these two attributes likely represent two independent phenomena. Therefore, it appeared probable that there exist specific interactions between the macromolecular substrate and the SK·HPN activator complex at the post-docking stage that play important role(s) in amplifying the relative low catalytic power associated with the two-domain constructs to that associated with the native tri-domain nSK, ones that are not being effectively utilized by the bi-domains despite a nearly native ability to dock the macromolecular substrate. If this were indeed true, one can further extend this model to assume that these interactions may either be short range, *i.e.* localized in and around the scissile peptide bond region in the catalytic domain of substrate HPG, or they could be relatively long range, such as those involving the kringle domains of substrate. Earlier studies on SK have provided a strong indication that kringle domains of substrate HPG do play an important role in HPG activation by nSK, because μPG, which is devoid of all the five kringle domains of HPG, both has significantly lowered affinity for the preformed SK·HPN activator complex (23) and is a poor substrate for activation (32). Thus, it is conceivable that both catalytic domain-centered as well as kringle domain-related interactions are operative together during substrate recognition and turnover by the SK·HPN activator complex. Hence, with a view to obtain insights into the relative contributions of different domains of substrate HPG (*i.e.* catalytic *versus* kringle domains), we compared the rates for activation of HPG by single-, bi-, and tri-domain structures with those for the isolated catalytic domain, using as substrate μPG (which also, like native full-

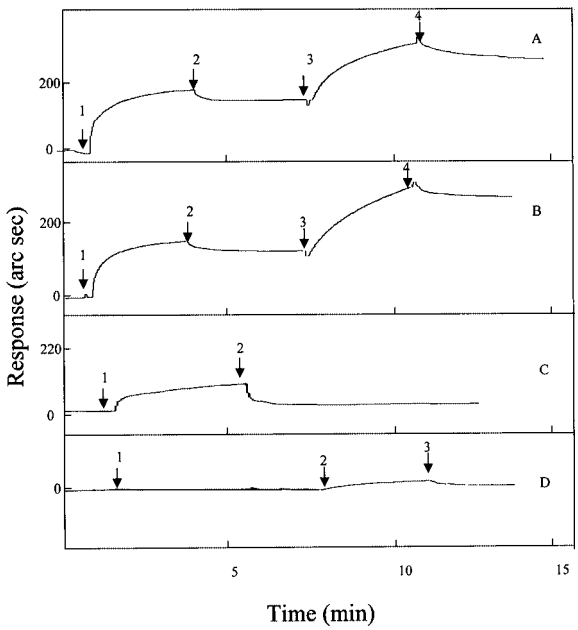

FIG. 3. **Composite pictures of IAsys™ Resonant Mirror-based real time kinetic analysis to explore the ternary interactions between substrate HPG and equimolar binary complex of nSK/SK domains and immobilized HPG.** The experiment was carried out at 25 °C in binding buffer as described under "Experimental Procedures." Human PG was biotinylated and immobilized on to a layer of streptavidin captured on the biotin cuvette surface. Stable binary complexes were then formed by adding saturating concentration of either nSK (500 nM, *A*), $\alpha\beta$ (500 nM, *B*), or α domain (1 μM, *C*) onto the immobilized HPG. The point of addition of nSK/SK domains (*viz.* nSK, *A*; $\alpha\beta$ domain, *B*; and α domain, *C*) in *A–C* is depicted by *arrows 1*. After washing with binding buffer (point of addition of binding buffer depicted by *arrow 2*), a stable dissociation base line (except in case of α domain, *D*) was rapidly obtained because of the high affinity and stability of the binary complexes. Thereafter, various concentrations of substrate HPG (0.1–1 μM) were added onto the binary complexes. However, for clarity in the figure, only a single (saturating) concentration of HPG (1 μM) is depicted (shown in *A* and *B* by *arrows 3*). The association phases were monitored for ~5 min, and subsequently the cuvettes were washed with the binding buffer (point of addition depicted in *A* and *B* by *arrows 4*). After each cycle of analysis in *A* and *B*, the undissociated substrate HPG was stripped off with 2.5 mM EACA, followed by re-equilibrating the cuvette with binding buffer, which re-established the original base line (data not shown). The nonspecific binding interaction between added substrate HPG with the HPG immobilized onto the cuvette in the absence of any SK/SK derivatives is depicted in *D* (*arrow 1* depicts the addition of binding buffer, *arrow 2* depicts the addition of HPG, and *arrow 3* depicts the dissociation of nonspecific HPG with the binding buffer). Note that the nonspecific signal was found to be less then 10% of the ternary signal in case of SK/SK derivatives. In a separate experiment the immobilized streptavidin alone was also taken as a negative control, and it was subjected to the same kind of treatments as given to the test cell containing immobilized HPG. Under these conditions no significant nonspecific binding was observed. Detailed protocols and rationale for these experiments are provided under "Experimental Procedures" and in Ref. 23.

length HPG, contains the scissile peptide bond but is devoid of all the kringle domains).

Interaction of μPG with nSK/SK Domains—Microplasminogen was generated from HPG by enzymatic cleavage with plasmin (see "Experimental Procedures" for details). Kinetic experiments were then performed using μPG as substrate and the different HPN-SK domain(s) as the activator species. The results demonstrated that in contrast to the activator activity of native SK·HPN with full-length HPG as substrate (taken as 100%), all the three types of SK structures (single-, bi-, and tri-domain) showed significantly low specific activity, ranging roughly over 1.0–2% when μPG was used as the substrate (see Table III for steady-state kinetic data). Interestingly, in general the K_m of nSK/SK domains for μPG was seen to be 4–5-fold lesser than that for full-length HPG, which at least partially accounts for the generally decreased specific activities observed when μPG was the substrate. However, these low activities against μPG could not be explained merely on the basis of their lowered affinity for the substrate because even at substrate saturation the activities of their HPN complexes remained essentially 40–50-fold lower as compared with that of SK·HPN against full-length HPG (Fig. 4). These results clearly establish that the co-factor activity of the various constructs against the kringle-less substrate could not be "compensated" by saturating the assays with substrate. Thus, the single- and two-domain constructs were likely truly compromised not just in terms of the substrate affinity but in terms of their catalytic power as well. It is therefore apparent that when kringles are "lost" from the macromolecular substrate, the catalytic advantage of even the native, three-domain SK becomes compromised, showing that the catalytic domain of macromolecular substrate is intrinsically a "poor" substrate for the SK·HPN activator complex. Another noticeable feature of the results is that for both the bi-domain derivatives of SK, the K_m for μPG was found to be nearly same as that of SK (~2.0 μM), whereas for the α domain there was an ~2-fold difference in K_m for μPG as compared with that of native SK (Tables II and III). This observation indicates the presence of additional, catalytic domain-specific substrate affinity in the two-domain constructs as compared with the single-domain derivative, α. The results also reveal that with μPG as substrate, the catalytic activity of the bi-domain construct $\alpha\beta$ (although exhibiting the generally lowered activity of all the constructs, including native SK, against the kringle-less substrate) was nearly 2-fold lower as compared with its activity against HPG (Tables I and III). This suggested that unlike the single domains, the two-domain constructs possessed an improved capability to interact with the kringles of substrate, resulting in a certain degree (although modest compared with the three-domain design) of catalytic enhancement, even though other indicators of enzyme-substrate interactions, such as K_m for substrate and direct, real time affinity measurements using Resonant Mirror analyses did not yield any definitive evidence providing a physico-chemical basis for this functional effect. However, it is clear from the steady-state kinetic studies that the binary complexes of nSK/SK domains (*i.e.* the tri- and bi-domains) interact with substrate μPG with essentially similar K_m, although in case of the α domain, the values are somewhat higher, indicating a relatively lowered substrate affinity. Remarkably, in all cases, even at saturating μPG concentrations, only poor co-factor activities compared with that of SK·HPN against full-length HPG were engendered. To directly validate these conclusions, real time binding parameters of ternary interactions between μPG and nSK/SK domains complexed to immobilized biotinylated-HPG were determined using the Resonant Mirror technique. The data (Table III), which are broadly consistent with the kinetics results, show that equilibrium dissociation constants (K_D) of ternary interaction between μPG and $\alpha\beta$ (~4.0 μM) and $\beta\gamma$ (~2.0 μM) were, at most, minimally different compared with that for nSK (~1.0 μM). Thus, these analyses suggest that the binary complexes of the bi-domains and the native, tri-domain nSK with HPG dock μPG with affinities that are not grossly different from each other. However, it is worth noting that as compared with the docking of substrate HPG onto the binary complexes of nSK/SK domains, μPG docks onto the latter with an affinity that is approximately an order of magnitude lower.

One of the main conclusions emerging from the present study is that kringle domains of HPG play an important role in docking of the macromolecular substrate onto the native acti-

TABLE III

Steady state kinetics and real time association-dissociation data for the HPN complex of SK/SK domains with substrate microplasminogen

Kinetic parameters of substrate μPG activation were determined at 22 °C spectrophotometrically after mixing with equimolar HPN. Binding data kinetic constants for substrate μPG interactions with nSK/SK domains and immobilized biotinylated HPG were determined by Resonant Mirror analysis using a IAsys Plus system, as explained under "Experimental Procedures." A stable binary complex between nSK/SK domains and immobilized HPG was first made on the reaction cuvette, and then the real time binding isotherms of varying concentrations of μPG (1–6 μM) were monitored.

Activator protein	K_m	k_{cat}	k_{cat}/K_m	k_a	k_d	K_D
	μM	min^{-1}	$min^{-1}\ \mu M^{-1}$	$M^{-1}\ s^{-1}$	s^{-1}	M
nSK	2.0 ± 0.5	0.26 ± 0.1	0.125	$0.3 \pm 0.1\times10^5$	$3.3 \pm 0.7\times10^{-2}$	$1.1 \pm 0.05\times10^{-6}$
αβ	2.5 ± 0.5	0.22 ± 0.1	0.088	$0.67 \pm 0.18\times10^5$	$2.7 \pm 0.5\times10^{-2}$	$4.07 \pm 1.5\times10^{-6}$
βγ	2.0 ± 0.5	0.20 ± 0.05	0.1	$0.13 \pm 0.06\times10^5$	$3.7 \pm 0.5\times10^{-2}$	$2.3 \pm 1.0\times10^{-6}$
α[a]	4.0 ± 1.0	0.15 ± 0.1	0.0375	ND[b]	ND	ND
β[a]	ND	ND	ND	ND	ND	ND

[a] In case of α and β the binding constants with substrate μPG could not be determined as the binary complexes of these isolated domains with immobilized HPG were intrinsically weak (see Table II) and tended to dissociate rapidly in the binding buffer itself. Thus, reliable estimates of any ternary complexation even if weak could not be made even at highest concentration of μPG (4 μM) added.

[b] ND, not detected.

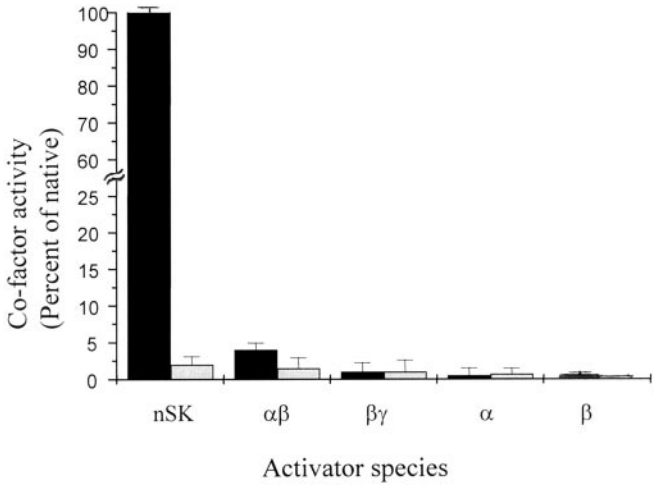

FIG. 4. **Comparison of substrate HPG and μPG activation capability of nSK/SK domains.** The histogram depicts the comparison of co-factor activity of SK, bi-domain constructs of SK (αβ and βγ), and single domain constructs (α and β); in all cases, activity was measured along with equimolar HPN for the activation of either of two macromolecular substrates, *i.e.* HPG and μPG. The saturating concentration of HPG used in case of tri- (nSK) and bi-domains (αβ and βγ) was 2 μM, whereas in case of single-domains (α and β) the co-factor activity was measured at 8 μM HPG. The co-factor activity of tri- (nSK) and bi-domains (αβ and βγ) was measured at saturating concentration of μPG (4 μM), whereas the co-factor activity of single-domains (α and β) was measured at 10 μM μPG. The percentage activity of different activator complexes was then calculated as a percentage value in comparison with the co-factor activity of SK·HPN when HPG was the substrate taken to be 100%. The histogram shows a maximal percentage of co-factor activity of different domains of SK against HPG (*black*) and μPG (*light gray*) at their respective saturating substrate concentrations. The data highlight the fact that of all the various constructs and substrate types, only the tri-domain motif was able to generate the full (100%) activity associated with native SK and full-length HPG, whereas all the other partial-length constructs with either substrate or even the native, three-domain SK with μPG as substrate were able to generate only a very low level of co-factor activity compared with SK·HPN and substrate HPG.

vator complex. However, although the macromolecular docking phenomenon is crucially important in generating nascent co-factor activity in the HPN active site, it is probably not the sole determinant of the "full-blown" co-factor activity associated with the native system, *viz.* SK·HPN *versus* HPG as the substrate. This conclusion is supported by the observation that both the two-domain derivatives, αβ and βγ, can dock HPG nearly as efficiently as the native activator complex (as indicated by their respective K_m and K_D values) but fail to generate native-like co-factor activity. In other words, the docking of substrate by the two bi-domain structures is native-like, yet their catalytic rates are a mere fraction of the rates seen with native SK and full-length HPG. Thus, it seems reasonable to conclude that it is only when all three domains of SK simultaneously present that the ability to exploit the kringle domains for improved catalytic rates (as opposed to "mere" improvement in substrate affinity) effectively gained. Thus, kringles help not only in docking substrate at the active site but also dramatically accelerate the rates of catalysis by the activator complex. The present studies strongly suggest that events subsequent to substrate docking, which require all three domains of native SK together with the kringle domain(s) of the substrate, are critical in the development of the full-blown catalytic activity of the SK·HPN activator enzyme, and although stereo-chemical positioning of the scissile peptide bond is necessary in conferring a native-like macromolecular specificity, it can generate limited catalytic turnover on its own, with the major jump in catalytic power being achieved through long range protein-protein interactions with substrate kringles. This mechanism of substrate-assisted proteolysis encountered in SK is clearly distinct from that of other direct HPG activators like tissue plasminogen activator and urokinase, which display catalysis with nearly the same rates irrespective of the presence or absence of kringles in the substrate.[2] However, of all these activators (including SAK), the catalytic power of the SK·HPN complex is recognized to be the highest (18, 34, 42), probably because of the recruitment of long range interactions between enzyme and its protein substrate in its catalytic mechanism of action. This may indeed be the underlying structural reason for the evolutionary selection of a three-domain activator design, particularly one in which specific interactions between the activator species and macromolecular substrate are centered not only on the target of proteolysis, the catalytic domain (which, by itself, is not surprising), but also with regions located far away from the site of enzymatic action by the active site *per se*. Although speculative at present, it seems plausible that the tri-domain molecule is able to optimally "sense" a signal during catalysis, probably conformational changes in the catalytic domain as the scissile peptide bond is cleaved, as well as the relatively large structural changes that are known to occur in the orientation of the kringles following the conversion of substrate plasminogen to plasmin (43, 44). This process, by facilitating the release of the product of the catalytic cycle from the active site, would help attain the native-like protein co-factor activities seen in the SK system. Further detailed studies are undoubtedly required now to elucidate the exact mech-

[2] J. S. Nanda and G. Sahni, unpublished observations.

anisms, for example those exploiting site-specific spectroscopic monitoring for fluorescence resonance energy transfer analysis to help probe the molecular motions during substrate capture, catalytic transformation, and, finally, product release. However, the results presented in this study, by illuminating the initial steps in an otherwise extremely complex biochemical reaction, unambiguously indicate that the substrate-specific proteolytic capability generated in the immediate vicinity of the HPN active site upon complexation with SK is amplified in a dramatic manner through long range, "supra-catalytic center-based" protein-protein interactions between the co-factor and macromolecular substrate. The elucidation of the exact molecular events and epitopes involved in this process would greatly help in the redesign of existing proteases into efficient substrate specific HPG activator enzymes and also in the future *de novo* design of novel target-specific proteolytic functionalities with useful applicability.

Acknowledgments—We thank Dr. Amit Ghosh, Director, for the facilities provided and support, Paramjit Kaur for expert technical assistance, and Dr. A. Pande for help in analysis of SPR data. Automated DNA sequencing was carried out with the unstinted help of Drs. Jagmohan Singh and K. Ganesan. We express our gratitude to Dr. Rajendra P. Roy (National Institute of Immunology, New Delhi) for the use of CD facilities. We thank Kamlesh Sharma and Dr. Sabita Basu of the Dept. of Hematology and the Blood Bank at the Government Medical College Hospital (Sector 32, Chandigarh) for providing us with human plasma.

REFERENCES

1. Castellino, F. J. (1981) *Chem. Rev.* **81,** 431–446
2. International Study of Infarct Survival-3 Collaborative Group (1992) *Lancet* **339,** 753–781
3. Conejero-Lara, F., Parrado, J., Azuaga, A. I., Smith, R. A. G., Ponting, C. P., and Dobson, C. M. (1996) *Protein Sci.* **5,** 2583–2591
4. Parrado, J., Conejero-Lara, F., Smith, R. A. G., Marshall, J. M., Ponting, C. P., and Dobson, C. M. (1996) *Protein Sci.* **5,** 693–704
5. Wang, X., Lin, X., Loy, J. A., Tang, J., and Zhang, X. C. (1998) *Science* **281,** 1662–1665
6. Christensen, L. R., (1947) *J. Gen. Physiol.* **30,** 465–470
7. McClintock, D. K., and Bell, P. H. (1971) *Biochem. Biophys. Res. Commun.* **43,** 694–702
8. Reddy, K. N., and Markus, G. (1972) *J. Biol. Chem.* **247,** 1683–1691
9. Markus, G., and Werkheiser, W. C. (1964) *J. Biol. Chem.* **239,** 2637–2643
10. Boxrud, P. D., Fay, W. P., and Bock, P. E. (2000) *J. Biol. Chem.* **275,** 14579–14589
11. Marder, V. J. (1993) *Blood Coagul. Fibrinolysis* **4,** 1039–1040
12. Esmon, C. T., and Mather, T. (1998) *Nat. Struct. Biol.* **5,** 933–937
13. Sottrup-Jensen, L., Clayes, H., Eajdel, M., Petersen, T. E., and Magnusson, S. (1978) *Prog. Chem. Fibrinol. Thrombol.* **3,** 191–209
14. Nihalani, D., Raghava, G. P. S., and Sahni, G. (1997) *Protein Sci.* **6,** 1284–1292
15. Nihalani, D., Kumar, R., Rajagopal, K., and Sahni, G. (1998) *Protein Sci.* **7,** 637–648
16. Parry, M. A. A., Fernandez-Catalan, C., Bergner, A., Huber, R., Hopfner, K.-P., Schlott, B., Gührs, K.-H., and Bode, W. (1998) *Nat. Struct. Biol.* **5,** 917–923
17. Parry, M. A. A., Zhang, X. C., and Bode, W. (2000) *Trends Biochem. Sci.* **25,** 53–59
18. Wohl, R. C., Summaria, L., and Robbins, K. C. (1980) *J. Biol. Chem.* **255,** 2005–2013
19. Shibata, H., Nagaoka, M., Sakai, M., Sawada, H., Watanabe, T., and Yokokura, T. (1994) *J. Biochem.* (*Tokyo*) **115,** 738–742
20. Johnsen, L. B., Poulsen, K., Kilian, M., and Petersen, T. E. (1999) *Infect. Immun.* **67,** 1072–1078
21. Johnsen, L. B., Rasmussen, L., Petersen, T., Etzerodt, M., and Fedosov, S. (2000) *Biochemistry* **39,** 6440–6448
22. Loy, J. A., Lin, X., Schenone, M., Castellino, F. J., Zhang, X. C., and Tang, J. (2001) *Biochemistry* **40,** 14686–14695
23. Dhar, J., Pande, A. H., Sundram, V., Nanda, J. S., Mande, S. C., and Sahni, G. (2002) *J. Biol. Chem.* **277,** 13257–13267
24. Lin, L.-F., Houng, A., and Reed, G. L. (2000) *Biochemistry* **39,** 4740–4745
25. Deutsch, D. G., and Mertz, E. T. (1970) *Science* **170,** 1095–1096
26. Studier, F. W., Rosenberg, A. H., Dunn, J. J., and Dubendorff, J. W. (1990) *Methods Enzymol.* **185,** 60–89
27. Chaudhary, A., Vasudha, S., Rajagopal, K., Komath, S. S., Garg, N., Yadav, M., Mande, S. C., and Sahni, G. (1999) *Protein Sci.* **8,** 2791–2805
28. Radek, J. T., and Castellino, F. J. (1989) *J. Biol. Chem.* **264,** 9915–9922
29. Jackson, K. W., Malke, H., Gerlach, D., Ferretti, J. J., and Tang, J. (1986) *Biochemistry* **25,** 108–114
30. Porath, J., Carlsson, J., Olsson, I., and Belfrage, G. (1975) *Nature* **258,** 598–599
31. Yang, J. T., Wu, C., and Martinez, H. M.(1986) *Methods Enzymol.* **130,** 208–269
32. Shi, G.-Y., and Wu, H.-L. (1988) *J. Biol. Chem.* **263,** 17071–17075
33. Chase, T., Jr., and Shaw, E. (1969) *Biochemistry* **8,** 2212–2224
34. Wohl, R. C., Arzadon, L., Summaria, L., and Robbins, K. C. (1977) *J. Biol. Chem.* **252,** 1141–1147
35. Cush, R., Cronin, J. M., Stewart, W. J., Maule, C. H., Molloy, J., and Goddard, N. J. (1993) *Biosensors Bioelectronics* **8,** 347–354
36. Buckle, P. E., Davies, R. J., Kinning, T., Young, D., Edwards, P. R., Pollard-Knight, D., and Lowe, C. R.(1993) *Biosensors Bioelectronics* **8,** 355–363
37. Myszka, D. G. (1997) *Curr. Opin. Biotech.* **8,** 50–57
38. Morton, T. A., Myszka, D. G., and Chaiken, I. M. (1995) *Anal. Biochem.* **227,** 176–185
39. Wang, X., Terzyan, S., Tang, J., Loy, J. A., Lin, X., and Zhang, X. (2000) *J. Mol. Biol.* **295,** 903–914
40. Wang, X., Tang, J., Hunter, B., and Zhang, X. C. (1999) *FEBS Lett.* **459,** 85–89
41. Wang, S., Reed, G. L., and Hedstrom, L. (1999) *Biochemistry* **38,** 5232–5240
42. Robbins, K. C., Summaria, L., and Wohl, R. C. (1981) *Methods Enzymol.* **80,** 379–387
43. Mangel, W. F., Lin, B. H., and Ramakrishnan, V. (1990) *Science* **248,** 69–73
44. Marshall, J. M., Brown, A. J., and Ponting, C. P. (1994) *Biochemistry* **33,** 3599–3606